Hindawi Publishing Corporation
Journal of Nanomaterials
Volume 2016, Article ID 9806386, 9 pages
http://dx.doi.org/10.1155/2016/9806386

Research Article

Influence of Surface Treatment and Annealing Temperature on the Recombination Processes of the Quantum Dots Solar Cells

Tung Ha Thanh,[1,2] Vinh Lam Quang,[3] and Huynh Thanh Dat[4]

[1]*Department for Management of Science and Technology Development, Ton Duc Thang University, Ho Chi Minh City, Vietnam*
[2]*Faculty of Applied Sciences, Ton Duc Thang University, Ho Chi Minh City, Vietnam*
[3]*University of Science, Vietnam National University, Ho Chi Minh City, Vietnam*
[4]*Vietnam National University, Ho Chi Minh City, Vietnam*

Correspondence should be addressed to Tung Ha Thanh; hathanhtung@tdt.edu.vn

Received 12 June 2016; Revised 31 August 2016; Accepted 4 September 2016

Academic Editor: Taeseup Song

We have studied the effect of the surface treatment of the CdS/CdSe quantum dots (QDs) by passivation ZnS layers and annealing temperature on the recombination resistance of the quantum dots solar cells (QDSSCs) based on TiO_2/CdS/CdSe/ZnS photoanodes. The recombination resistance at TiO_2/QDs contact and in TiO_2 film decreased when the QDs were added to the passivation ZnS layers. Furthermore, we used the F^- ions linker and found the best annealing temperature conditions to reduce the recombination resistance of the QDSSCs. As a result, the current density increased from 7.85 mA/cm^2 to 14 mA/cm^2.

1. Introduction

Recently, the scientists in the world have been interested in the QDSSCs based on the TiO_2 substrate. The QDSSCs based on the QDs have more advantages than the dye sensitized solar cells (DSSCs) based on the molecules for some reasons: (1) the molecules only absorb the light in visible region (2) and are unstable in the air environment. Beside the disadvantages of the molecules, the QDs have some advantages such as quantum confinement effect, the higher coefficients than the dyes, and the generation of multiple electron-hole pairs by a single incident photon [1, 2]. Moreover, the tunable adsorption band of the QDs can be performed by changing their size for the light harvesters in QDSSCs [3].

For those reasons, the QDSSCs were promised to become the candidate for the high efficiency. Firstly, Vogel and colleagues prepared the QDSSCs based on CdS QDs and obtained the low efficiency [4]. In 2008, many scientists only studied the single QDs as CdS, CdSe, PbS, and so on for the application in the QDSSCs. Therefore, the results obtained the low efficiency. For the next years, the series articles focus on improving efficiency of the QDSSCs with the subject to improve the adsorption of the photoanodes [5, 6]; to use the different methods such as chemical bath deposition (CBD), successive ionic layer adsorption, and reaction (SILAR) [7]; and to apply the core-shell QDs to reduce the surface states in the QDs [8]. However, the efficiency of the QDSSCs was still lower than the efficiency of the DSSCs at the present due to the high surface states at the TiO_2/QDs contact and the large diffusion resistance in the TiO_2 film.

In this article, we studied the influence of the surface treatment processes by the passivation ZnS coating and the annealing temperature on the recombination resistance of the QDSSCs based on the TiO_2/CdS/CdSe/ZnS photoanodes.

2. Experiments

2.1. CdSe QDs Synthesis. The CdSe QDs were prepared using colloidal synthesis as detailed by previous work [9].

2.2. Growth of TiO_2/CdS/CdSe/ZnS Photoanodes. FTO (Figure 1) was coated with TiO_2 films by doctor blade method and annealed at 500°C for 45 minutes. Next, the film was immersed in 40 mmol $TiCl_4$ solution for 30 minutes at 70°C and sintered at 300°C for 15 minutes, 400°C for 15 minutes, 450°C for 15 minutes, and 500°C for 30 minutes to avoid the breaking films.

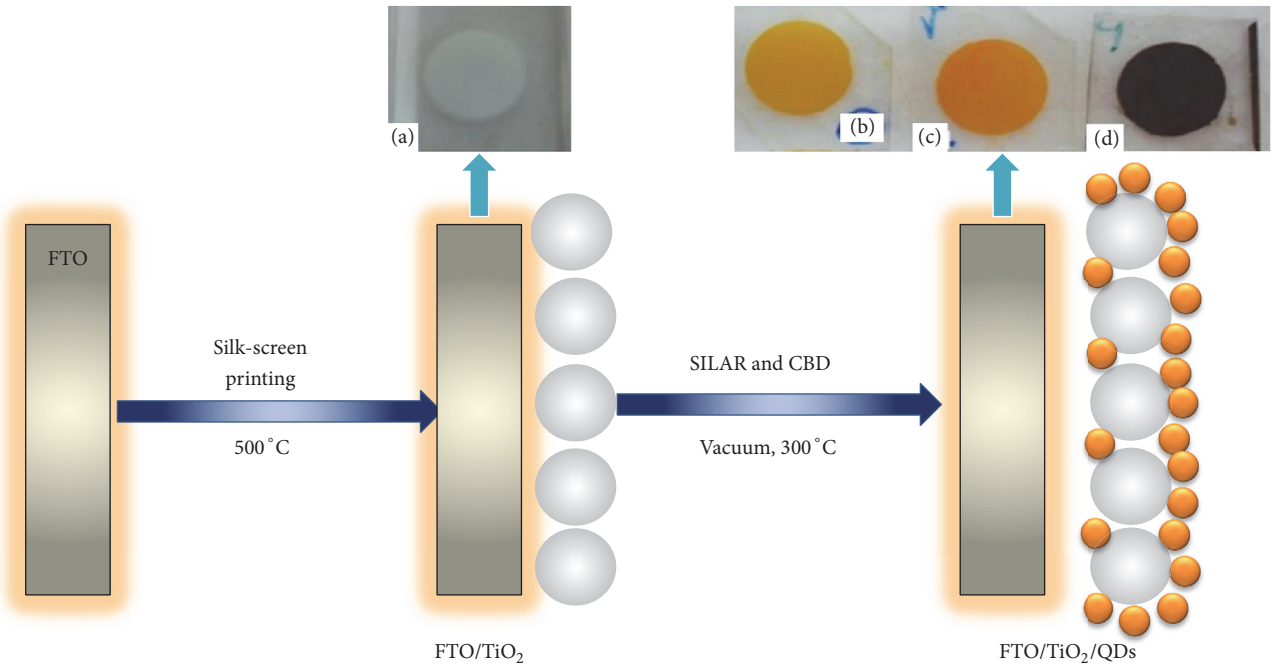

Figure 1: Schematic of the structural photoanode.

Firstly, the FTO/TiO_2 films were immersed into 0.5 M Cd^{2+}-ethanol solutions and 0.5 M S^{-}-methanol for 1 minute. After, film was rinsed with methanol and ethanol before being dried in air (a SILAR cycle). The immersion cycle was repeated three times for CdS layers. Secondly, the TiO_2/CdS assembly was immersed into the CdSe solution (size ~3-4 nm) for 24 hours before being dried at room temperature. Thirdly, the TiO_2/CdS/CdSe film was immersed into 0.1 M Zn^{2+} and 0.1 M S^{2-}-solutions for 1 minute and rinsed with pure water (a SILAR cycle). The immersion cycle was repeated two times for ZnS layers. Finally, the TiO_2/CdS/CdSe/ZnS photoanodes were annealed in vacuum at 300°C to prevent oxidation.

The coating of F^{-} ions was performed by dipping the TiO_2 photoelectrode into a 1 M NH_4F aqueous solution for 5 min, rinsed by deionized water 1 min. Two layers of F^{-} ions were coated: the first was coated before the deposition of CdS QDs, the second after the deposition of CdS QDs, and the third after the deposition of CdSe QDs [10].

2.3. Electrolyte Solution. The electrolyte was prepared by the mix of 0.5 M Na_2S, 0.2 M S, and 0.2 M KCl solutions in Milli-Q ultrapure water/methanol (7 : 3 by volume) [9].

2.4. Characterization. The morphological samples were investigated using the transmission electron microscopy (TEM). The crystal structure was analyzed using an X-ray diffractometer (XRD) (Philips, PANalytical X'Pert, CuK_α radiation). The absorption properties of the samples were investigated using a diffusive reflectance UV-Vis spectrometer (JASCO V-670). Photocurrent-voltage measurement was from Solarena, Sweden, which has performed on a Keithley 2400 source meter using a simulated AM 1.5 sunlight with an output power of 100 mW/cm^2 produced by a solar simulator. The Electrochemical Impedance Spectroscopy (EIS) was carried out on ZAHNER IM6e Electrochemical Workstations over a frequency range 0.1–10^5 Hz at zero bias voltage.

3. Results and Discussions

3.1. Morphological and Structure Analysis of the TiO_2/CdS/CdSe/ZnS Photoanodes. To obtain the particles size, the TEM image of the TiO_2/CdS/CdSe/ZnS photoanode was investigated. Figure 2(a) presents the TEM image of the TiO_2/CdS/CdSe/ZnS photoanode annealed at 300°C in vacuum with the 5 nm size of the QDs. The structure of the photoanodes can be studied by the Raman in Figure 2(b). It indicates that the photoanode has the crystalline structure of Anatase phase with the modes at 144 cm^{-1}, 397 cm^{-1}, 517 cm^{-1}, and 638.5 cm^{-1} [11]. Moreover, the Raman also have the 1LO (long optic) and 2LO modes of the CdSe QDs at 206,5 cm^{-1}, and 405 cm^{-1}; LO mode of the CdS QDs at 298 cm^{-1}; and LO mode of the passivation ZnS layers at 364 cm^{-1} [12]. These results show that the CdS, CdSe, and ZnS particles were deposited on the TiO_2 film.

Beside the Raman, the structural TiO_2/CdS/CdSe/ZnS photoanodes are also considered by the XRD patterns. Figure 2(c) indicates that the TiO_2 films have the crystalline structure of the Anatase phase (JCPDS 21-1272) with the strong peak at 25,4° corresponding to the (101) plane. This result indicates that the growth of the TiO_2 film follows the crystal axis [13]. In addition, the XRD patterns also showed that the three peaks at 26,4°, 44°, and 56,1° correspond to (111), (220), and (311) planes of the CdS, CdSe, and ZnS cubic (JCPDS 41-1049, JCPDS 65-2891, and JCPDS 05-0566) [14–16].

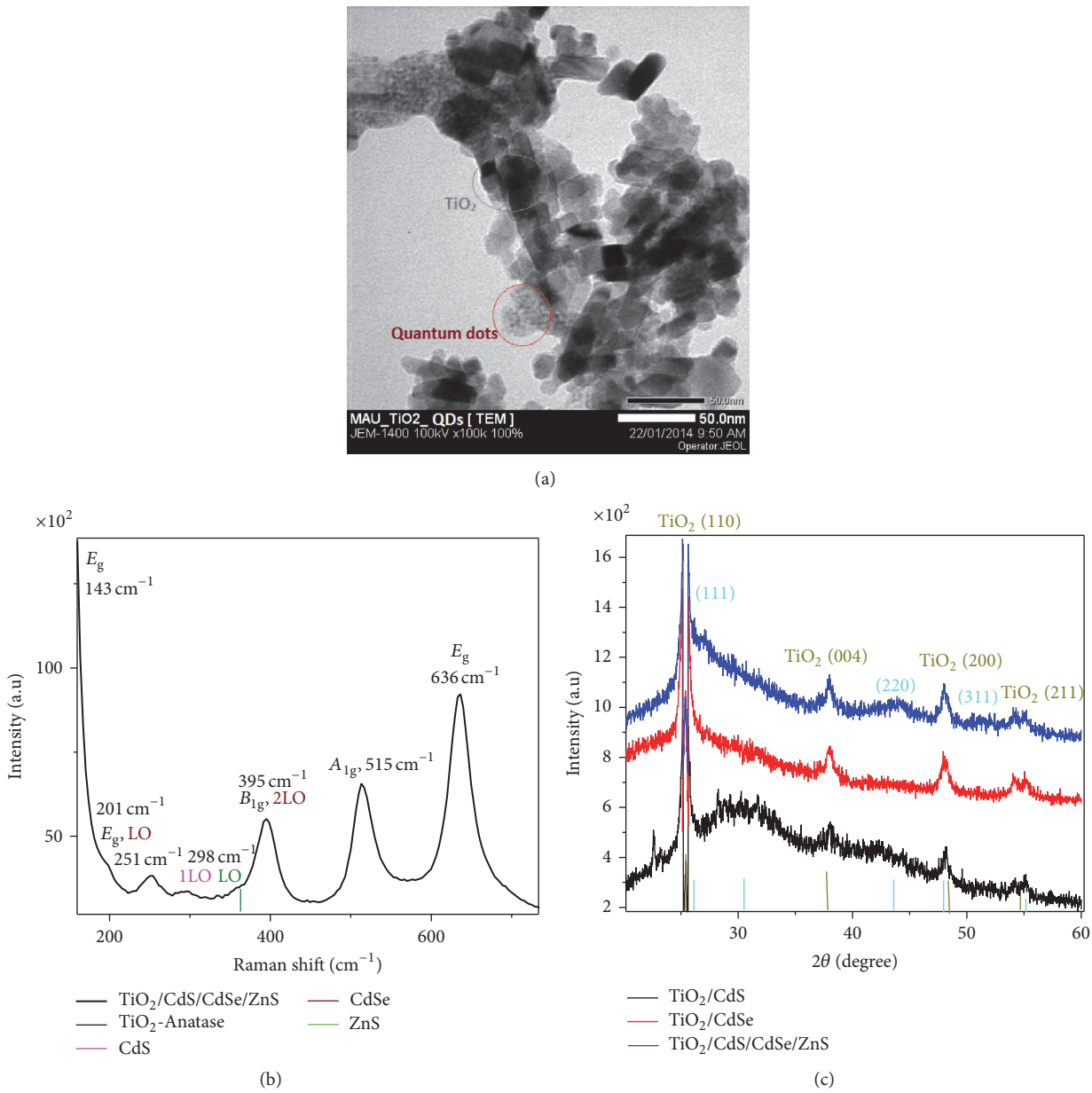

Figure 2: (a) The TEM image, (b) Raman spectra, and (c) XRD patterns of the different photoanodes annealed in vacuum.

3.2. Influence of the Surface Treatment. The combination of the two types QDs can increase the intensity of the absorption of the photoanodes to improve the high performance of the QDSSCs [5, 17, 18]. However, the efficiency of the QDSSCs is still lower than the efficiency of the DSSCs due to the high recombination processes at TiO_2/QDs contact and the diffusion into the TiO_2 film. Therefore, the ZnS passivation layers were coated on the surface of the CdS/CdSe QDs to reduce the recombination processes and the black electrons into the electrolyte.

Figure 3(a) is the UV-Vis of the different photoanodes to depend on the ZnS passivation layers. As expected, when thickness of the ZnS passivation increased, the intensity of the UV-Vis also increased due to the more ZnS particles loading on the photoanodes [19]. This result is good for the investigation to the influence of the ZnS passivation thickness on the recombination resistance of the QDSSCs.

To determine the effect of the ZnS thickness on the recombination resistance of the QDSSCs, we considered the *I-V* curves of the QDSSCs based on the different photoanodes. Figure 3(b) shows the *I-V* curves of the QDSSCs with or without the ZnS passivation coating (*an active area 0.38 cm²*) at AM 1.5 (*100 mW/cm²*). In this work, the thickness of the ZnS layers changed from 0 to 5 layers as shown in Table 1. The QDSSCs based on the TiO_2/CdS/CdSe/ZnS (2 layers) photoanodes have the open voltage (V_{OC}) ~ 0.44 V, the current density (J_{SC}) ~ 14 mA/cm², the fill factor ~0.41, and the efficiency

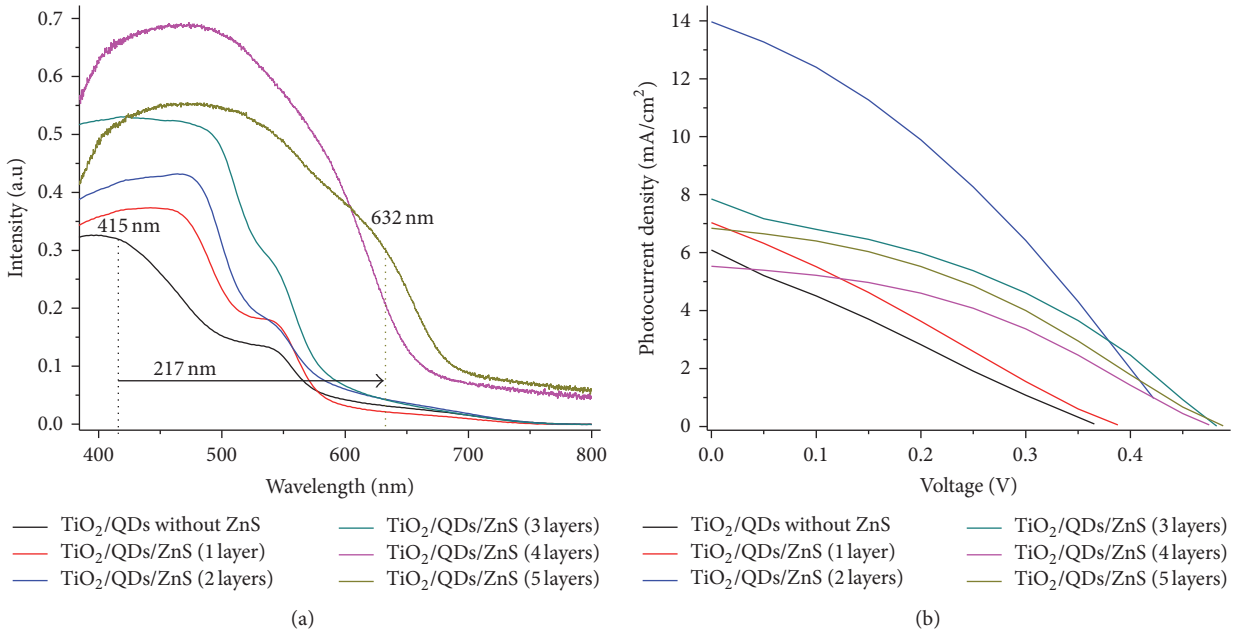

Figure 3: (a) The UV-Vis spectra and (b) I-V curves of the QDSSCs with the different photoanodes.

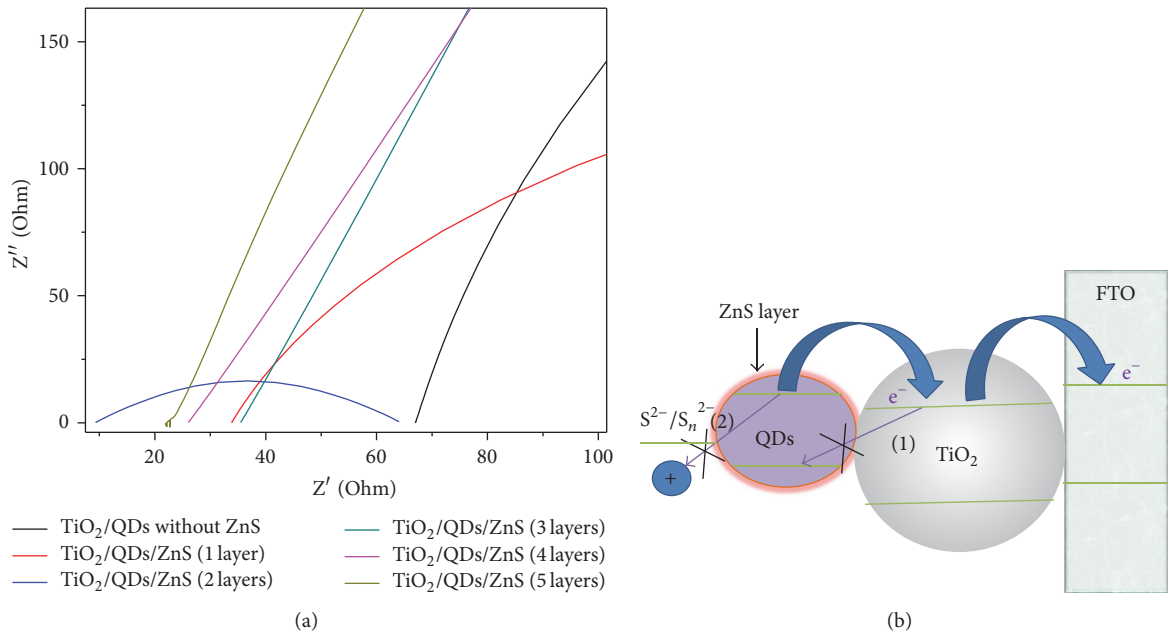

Figure 4: (a) Nyquist plots measured under illuminated conditions for the QDSSCs with the different photoanodes and (b) diagram of the recombination routes for photoelectrons.

(η) ~ 2.1%. This result indicates that the efficiency of the QDSSCs based on the photoanodes with the ZnS passivation coating is higher than the efficiency of the QDSSCs based on the photoanodes without the ZnS passivation coating. This result agrees well with the UV-Vis spectra. To explain the reasons why the current density increased from 6.04 mA/cm^2 to 14 mA/cm^2, we used the diagram of the recombination routes for photoelectrons in Figure 4(b). The QDSSCs based on the photoanodes without the ZnS passivation layers can occur in the high recombination processes between the photoelectrons in the conduction band (CB) of the TiO$_2$ with the holes in the valence band (VB) of the CdS/CdSe QDs *(process 1)* and the holes in the electrolyte *(process 2: the back photoelectrons into electrolyte)*. When the CdS/CdSe QDs were coated with the ZnS passivation layers, the QDSSCs can be reduced in the recombination processes (1) and (2) in

Table 1: Photovoltaic performance parameters of the QDSSCs.

Number	QDSSCs	J_{SC} (mA/cm^2)	V_{OC} (V)	Fill factor FF	Efficiency η (%)
1	TiO_2/CdS/CdSe without ZnS	6.04	0.35	0.255	0.54
2	TiO_2/CdS/CdSe/ZnS (1 layer)	7.03	0.39	0.26	0.72
3	TiO_2/CdS/CdSe/ZnS (2 layers)	14	0.44	0.33	2.1
4	TiO_2/CdS/CdSe/ZnS (3 layers)	7.85	0.48	0.36	1.38
5	TiO_2/CdS/CdSe/ZnS (4 layers)	6.8	0.488	0.29	1.2
6	TiO_2/CdS/CdSe/ZnS (5 layers)	5.53	0.475	0.27	1.0

Table 2: The values of parameters were obtained from the EIS measurements.

Number	QDSSCs	R_S (Ω)	R_{ct2} (Ω)	R_{ct1} (Ω)	τ (ms)	C_μ (μF)
1	TiO_2/CdS/CdSe without ZnS	67	1190	268	4.9	104
2	TiO_2/CdS/CdSe/ZnS (1 layer)	33.8	333	158	3.2	428
3	TiO_2/CdS/CdSe/ZnS (2 layers)	9.24	41.6	13.5	2.13	1040
4	TiO_2/CdS/CdSe/ZnS (3 layers)	35.4	1930	2330	1.6	35.4
5	TiO_2/CdS/CdSe/ZnS (4 layers)	22.6	976	12000	1.9	28.5
6	TiO_2/CdS/CdSe/ZnS (5 layers)	26	59000	16100	2.2	46.4

Figure 4(b) [20]. The results show that the current density and the efficiency of the QDSSCs increased. Moreover, the optimal thickness of the photoanode with the ZnS layers is 2 layers. The efficiency of the QDSSCs decreased when the thickness of the ZnS passivation layers increased due to the high recombination processes when the ZnS particles were more loading on the photoanodes [19].

The EIS using for the QDSSCs was found by Mora-Sero group [21]. The EIS were used for investigation of the transfer processes of photoelectrons through the contacts and diffusion into the TiO_2 film such as pumping the photoelectrons from the CdS, CdSe QDs to the CB of the TiO_2; diffusion of the photoelectrons in the TiO_2 film; and recombination of the photoelectrons with electrolyte. All processes were described by the circuit diagrams obtained from the Fit and Simulator software of the EIS. After obtaining the EIS, the Nyquist of the circuit diagrams was fitted with the Nyquist of the experiment. At first, we chose the circuit diagrams in the Fit and Simulator software such as resistance, capacitance, and phase element to sign the circuit diagrams. After fitting, we can determine the parameters such as R_S, R_{ct1}, R_{ct2} in Table 2. The QDSSCs were illuminated by the Simulator with the power 150 W, at 1000 W/m^2.

Figure 4(a) shows the EIS of the QDSSCs based on the TiO_2/CdS/CdSe/ZnS photoanodes with the ZnS passivation layers changed from 0 to 5 layers. The Nyquist has the three semicircles at the different frequencies. The first semicircle *(from left to right in the Figure 4(a))* at the high frequencies *(95 Hz–1000 kHz)* corresponds to the transfer of electrons through the Pt/electrolyte contact and FTO/TiO_2 contact *(note R_{tc1})*. The second semicircle at the middle frequencies *(0.44–95 Hz)* shows the resistance against electrons diffusion into the TiO_2 films and the resistance against the transfer electrons through the TiO_2/QDs/electrolyte contact *(note R_{ct2})*. The third semicircle at the low frequencies *(0.049–0.44 Hz)* is due to the electrons diffusion in S_n^{2-}/S^{2-}.

In Figure 4(a), the radius of semicircles was extended when the thickness of the ZnS passivation layers increased. In addition, samples 2 and 3 still show the morphology of the three semicircles. However, when the thickness of the ZnS passivation layers increased, semicircles 1 and 3 were mixed up with semicircles 2. Therefore, we only discussed the semicircle at the middle frequencies. When the layers of the ZnS changed from 1 to 2, the radius of semicircles was narrow *(R_{ct2} from 1190 to 41.6 Ω)* due to the increased concentration of the photoelectrons through the TiO_2 film and the TiO_2/QDs/electrolyte contact [19]. However, the radius of the semicircle increased when the layers of the ZnS were over 3 layers *(R_{ct2} from 41.6 to 59000 Ω)*. These results indicate that the resistance against the electrons diffusion into the TiO_2 film increased [15, 19].

Besides the recombination resistance, the chemical capacitance correlates with the electrons concentration in the TiO_2 CB were determined from the EIS, $C_\mu \infty \exp(qV_F/k_BT)$, where q is the elementary charge, k_B is Boltzmann constant and T is the Kelvin temperature, V_F is the difference between the quasi-Fermi level at bias and the equilibrium, and $V_F = (E_{Fn} - E_{F0})/q$. C_μ is as a function of V_F. Therefore, we can determine the electrons concentration in the TiO_2 film when QDSSCs were illuminated. In Table 2, the chemical capacitance of the QDSSCs increased corresponding to the increased electrons concentration in the CB of the TiO_2 film when the CdS/CdSe QDs were coated with the ZnS passivation layers. These results agree well with the *I-V* curves and the Nyquist of the QDSSCs. With the ZnS passivation layers, we can reduce the recombination processes 1 and

Table 3: Photovoltaic performance parameters of the QDSSCs.

Number	QDSSCs	J_{SC} (mA/cm^2)	V_{OC} (V)	Fill factor FF	Efficiency η (%)
1	TiO_2/CdS/CdSe/ZnS at 100°C	5.73	0.38	0.3	0.67
2	TiO_2/CdS/CdSe/ZnS at 200°C	4.78	0.76	0.41	1.5
3	TiO_2/CdS/CdSe/ZnS at 300°C	14	0.44	0.33	2.1
4	TiO_2/CdS/CdSe/ZnS at 400°C	3.04	0.456	0.32	0.44

Table 4: The values of parameters were obtained from the EIS measurements.

Number	QDSSCs	R_S (Ω)	R_{ct2} (Ω)	R_{ct1} (Ω)	τ (ms)	C (μF)
1	TiO_2/CdS/CdSe/ZnS at 100°C	26.9	393	268	1.59	39.7
2	TiO_2/CdS/CdSe/ZnS at 200°C	33.8	333	158	1.82	52.6
3	TiO_2/CdS/CdSe/ZnS at 300°C	9.24	41.6	13.5	2.13	1040
4	TiO_2/CdS/CdSe/ZnS at 400°C	21.7	1160	1610	4.6	39.7

2 in Figure 4(b). The current density increased because the injected electrons into the CB of the TiO_2 increased. These results agree well with Jung and Jie group as the PbS and CdS QDs are coated with the ZnS passivation layers for reducing the recombination processes in the QDSSCs [22, 23].

Mora-Sero said that the recombination processes through the surface states of the QDs were enhanced in the QDSSCs [19]. Moreover, the recombination pathways in the QDSSCs also occurred in the CdS center and between the TiO_2 electrons and electrolyte [20]. Therefore, the recombination resistance reduced corresponding to the decreased recombination rate between the TiO_2 and electrolyte resulting in the enhanced electrons collection efficiency when the ZnS passivation layers were coated with the CdS/CdSe QDs in our experiments. These obtained results agree well with the results of Zhang et al. [19, 24]. Moreover, the enhanced electrons concentrations in the TiO_2 CB have been determined to the chemical capacitance valued in Table 2. The chemical capacitance increased when the ZnS layers coated correspond to the enhanced electrons efficiency in the QDSSCs [24].

3.3. Influence of Annealing Temperature. For improving the crystalline structure of the photoanodes, increasing the ability to the absorbers of light and the electrons transfer [20], we studied the QDSSCs based on the photoanodes at the different temperatures. At first, the photoanodes were annealed in the air environment where the CdS/CdSe QDs were oxidized. Therefore, all samples in this article were annealed in the vacuum. To determine the structure of the material after manufacture, we used XRD patterns. Figure 5(a) is XRD patterns of the photoanodes at different annealing temperatures. The structural analysis of the photoanodes at different annealing temperatures is similar to the analysis from Figure 2(a). The results indicate the TiO_2 Anatase, CdS, CdSe, and ZnS QDs with cubic. Moreover, when the temperature rose from 100°C to 400°C the XRD intensity increasing with the crystallization proved stronger in the crystal. Figure 5(b) shows the UV-Vis of the photoanodes at the different temperatures. At the high temperature, the peak of the UV-Vis shifted toward the long waves corresponding to the increased size. However, at 400°C, the CdS, CdSe, and ZnS concentrations of the photoanodes were burned and made the CdO. Therefore, the intensity of the UV-Vis spectra was decreased.

The parameters of the *I-V* curves *(Figure 5(c))* were obtained in Table 3. The QDSSCs based on the photoanodes annealed at 300°C have the highest efficiency. These results agree well with the UV-Vis. When the temperature increased, the photoanodes were the good crystallization *(reduced the recombination processes)* corresponding to the shifting toward the long waves. The results indicate that the current density increased because of the high electrons concentration in the TiO_2 CB. These results agree well with Yu group when the temperatures changed from 100°C to 250°C and the efficiency of the QDSSCs increased from 0.46% to 2.8% [8].

To confirm these obtained results in our experiments, the EIS were used for investigation of the recombination resistance and chemical capacitance of the QDSSCs. Figure 6 shows Nyquist plots measured under illuminated conditions for the QDSSCs based on the photoanodes at the different temperatures and (b) the image zoom of (a) *(inset)*. The values of parameters were obtained from the EIS measurements from Table 4. The result indicates that the recombination resistance decreased while the chemical capacitance increased at the high temperature (shown in Table 4). We noted that the decreased surface states and the enhanced electrons concentration in the TiO_2 CB were due to the perfected structural crystal at 300°C. These results agree well with the *I-V* characteristic.

4. Conclusions

We have successfully prepared the QDSSCs based on the TiO_2/CdS/CdSe photoanodes with the ZnS passivation layers

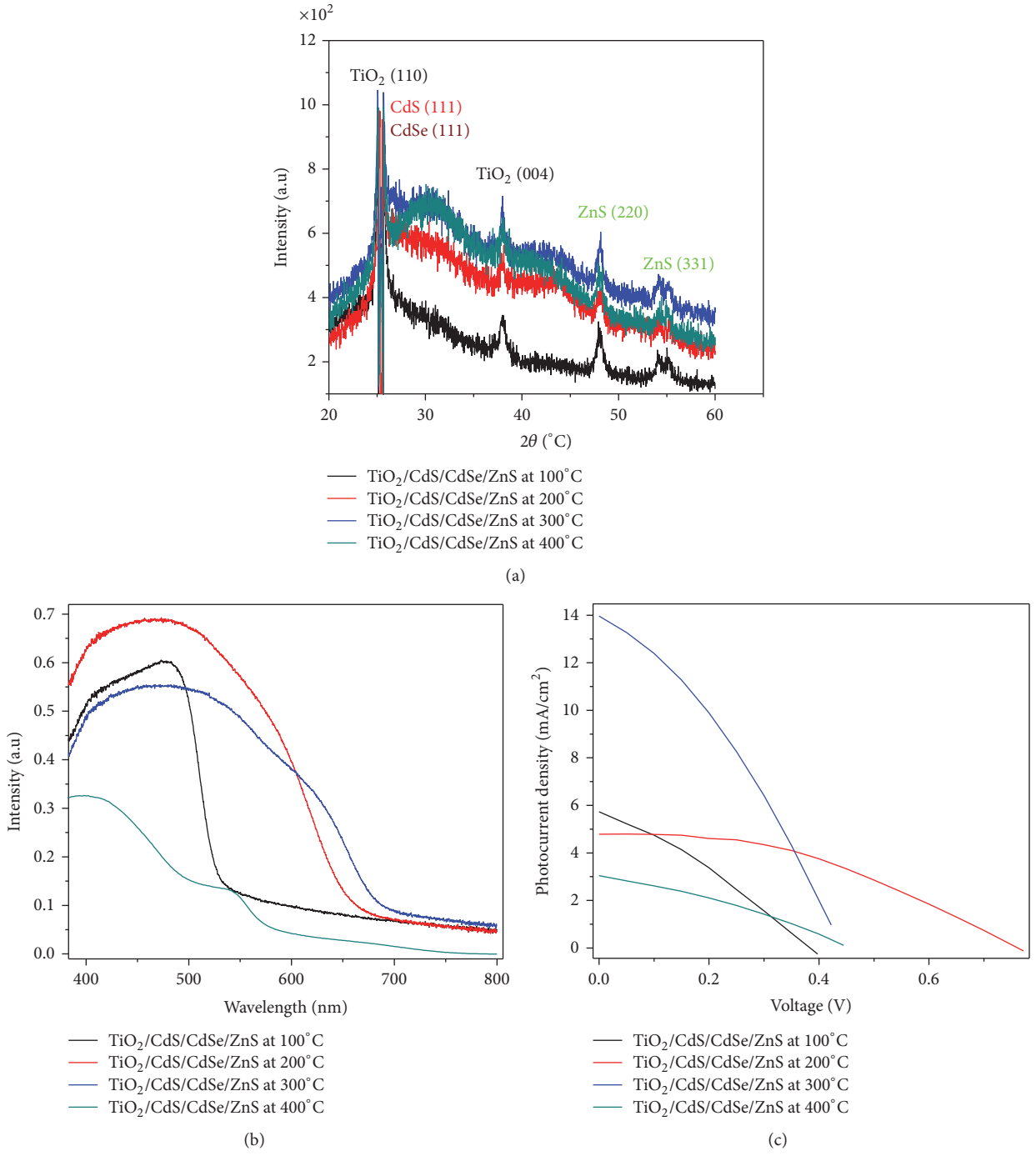

FIGURE 5: (a) XRD patterns of the photoanodes at the different annealing, (b) the UV-Vis, and (c) *I-V* curves of the QDSSCs based on the photoanodes at the different temperatures.

and influence of the annealing temperature on the recombination resistance of the QDSSCs. The recombination resistance of the QDSSCs decreased when the photoanodes were coated with the ZnS passivation layers. In addition, the current density and the electrons concentration in the TiO_2 CB increased due to the increased chemical capacitance. Beside, we also investigated the effect of the annealing temperature on recombination resistance, the chemical capacitance of the QDSSCs. The result shows that the crystallization structure perfected and reduced the recombination processes in the QDSSCs and the increased electrons concentration into the TiO_2 films.

Competing Interests

The authors have no competing interests to declare.

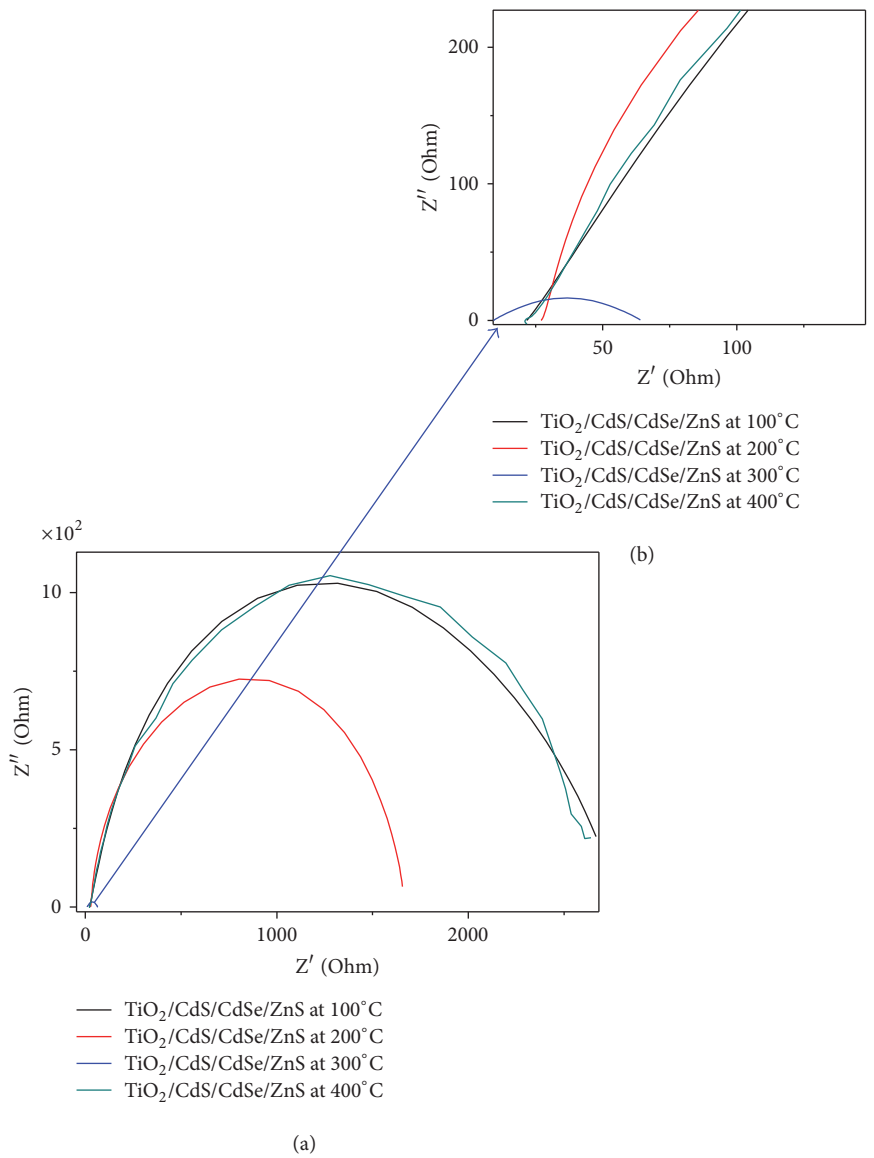

FIGURE 6: (a) Nyquist plots measured under illuminated conditions for the QDSSCs based on the photoanodes at the different temperatures and (b) small image *(inset)*.

Acknowledgments

This research is supported by Project CS2015.01.39. The authors would like to thank Ho Chi Minh City of Science, Vietnam. The authors would also like to thank Dr. Dang Vinh Quang for English language editing of the paper.

References

[1] A. J. Nozik, "Exciton multiplication and relaxation dynamics in quantum dots: applications to ultrahigh-efficiency solar photon conversion," *Inorganic Chemistry*, vol. 44, no. 20, pp. 6893–6899, 2005.

[2] J. Wu and Z. M. Wang, *Quantum Dot Solar Cells*, vol. 15, Springer, New York, NY, USA, 2014.

[3] P. Guyot-Sionnest, "Colloidal quantum dots," *Comptes Rendus Physique*, vol. 9, no. 8, pp. 777–787, 2008.

[4] R. Vogel, K. Pohl, and H. Weller, "Sensitization of highly porous, polycrystalline TiO_2 electrodes by quantum sized CdS," *Chemical Physics Letters*, vol. 174, no. 3-4, pp. 241–246, 1990.

[5] Y.-L. Lee and Y.-S. Lo, "Highly efficient quantum-dot-sensitized solar cell based on co-sensitization of CdS/CdSe," *Advanced Functional Materials*, vol. 19, no. 4, pp. 604–609, 2009.

[6] Q. Zhang, Y. Zhang, S. Huang et al., "Application of carbon counterelectrode on CdS quantum dot-sensitized solar cells (QDSSCs)," *Electrochemistry Communications*, vol. 12, no. 2, pp. 327–330, 2010.

[7] J. Chen, D. W. Zhao, J. L. Song et al., "Directly assembled CdSe quantum dots on TiO_2 in aqueous solution by adjusting pH value for quantum dot sensitized solar cells," *Electrochemistry Communications*, vol. 11, no. 12, pp. 2265–2267, 2009.

[8] X.-Y. Yu, B.-X. Lei, D.-B. Kuang, and C.-Y. Su, "High performance and reduced charge recombination of CdSe/CdS quantum dot-sensitized solar cells," *Journal of Materials Chemistry*, vol. 22, no. 24, pp.12058–12063, 2012.

[9] T. Ha Thanh, V. Lam Quang, and D. Huynh Thanh, "Determination of the dynamic resistance of the quantum dots solar cells by one I-V curve and electrochemical impedance spectra," *Solar Energy Materials and Solar Cells*, vol. 143, pp. 269–274, 2015.

[10] M. Samadpour, P. P. Boix, S. Giménez et al., "Fluorine treatment of TiO_2 for enhancing quantum dot sensitized solar cell performance," *Journal of Physical Chemistry C*, vol. 115, no. 29, pp. 14400–14407, 2011.

[11] A. Tubtimtae and M.-W. Lee, "Effects of passivation treatment on performance of CdS/CdSe quantum-dot co-sensitized solar cells," *Thin Solid Films*, vol. 526, pp. 225–230, 2012.

[12] J. Y. Kim, S. B. Choi, J. H. Noh et al., "Synthesis of CdSe-TiO_2 nanocomposites and their applications to TiO_2 sensitized solar cells," *Langmuir*, vol. 25, no. 9, pp. 5348–5351, 2009.

[13] G. I. Koleilat, L. Levina, H. Shukla et al., "Efficient, stable infrared photovoltaics based on solution-cast colloidal quantum dots," *ACS Nano*, vol. 2, no. 5, pp. 833–840, 2008.

[14] M. Kouhnavard, S. Ikeda, N. A. Ludin et al., "A review of semiconductor materials as sensitizers for quantum dot-sensitized solar cells," *Renewable and Sustainable Energy Reviews*, vol. 37, pp. 397–407, 2014.

[15] J.-H. Ahn, R. S. Mane, V. V. Todkar, and S.-H. Han, "Invasion of CdSe nanoparticles for photosensitization of porous TiO_2," *International Journal of Electrochemical Science*, vol. 2, no. 7, pp. 517–522, 2007.

[16] A. Kongkanand, K. Tvrdy, K. Takechi, M. Kuno, and P. V. Kamat, "Quantum dot solar cells. Tuning photoresponse through size and shape control of CdSe-TiO_2 architecture," *Journal of the American Chemical Society*, vol. 130, no. 12, pp. 4007–4015, 2008.

[17] P. Sudhagar, J. H. Jung, S. Park et al., "The performance of coupled (CdS:CdSe) quantum dot-sensitized TiO_2 nanofibrous solar cells," *Electrochemistry Communications*, vol. 11, no. 11, pp. 2220–2224, 2009.

[18] Z. Yu, Q. Zhang, D. Qin et al., "Highly efficient quasi-solid-state quantum-dot-sensitized solar cell based on hydrogel electrolytes," *Electrochemistry Communications*, vol. 12, no. 12, pp. 1776–1779, 2010.

[19] Y. Zhang, J. Zhu, X. Yu, J. Wei, L. Hu, and S. Dai, "The optical and electrochemical properties of CdS/CdSe co-sensitized TiO_2 solar cells prepared by successive ionic layer adsorption and reaction processes," *Solar Energy*, vol. 86, no. 3, pp. 964–971, 2012.

[20] L.-W. Chong, H.-T. Chien, and Y.-L. Lee, "Assembly of CdSe onto mesoporous TiO_2 films induced by a self-assembled monolayer for quantum dot-sensitized solar cell applications," *Journal of Power Sources*, vol. 195, no. 15, pp. 5109–5113, 2010.

[21] I. Mora-Seró, S. Giménez, T. Moehl et al., "Factors determining the photovoltaic performance of a CdSe quantum dot sensitized solar cell: the role of the linker molecule and of the counter electrode," *Nanotechnology*, vol. 19, no. 42, Article ID 424007, 2008.

[22] S. W. Jung, J.-H. Kim, H. Kim, C.-J. Choi, and K.-S. Ahn, "ZnS overlayer on in situ chemical bath deposited CdS quantum dot-assembled TiO_2 films for quantum dot-sensitized solar cells," *Current Applied Physics*, vol. 12, no. 6, pp. 1459–1464, 2012.

[23] J. Jiao, Z.-J. Zhou, W.-H. Zhou, and S.-X. Wu, "CdS and PbS quantum dots co-sensitized TiO_2 nanorod arrays with improved performance for solar cells application," *Materials Science in Semiconductor Processing*, vol. 16, no. 2, pp. 435–440, 2013.

[24] J. S. Woo, K. Jae-Hong, K. Hyunsoo, C. Chel-Jong, and A. Kwang-Soon, "Enhanced electron lifetime in CdS quantum dot-sensitized solar cells with nanoporous-layer-covered TiO_2 nanotube arrays," *Current Applied Physics*, vol. 12, no. 6, pp. 1459–1464, 2012.